

Cite this: *J. Mater. Chem. A*, 2018, 6, 6931

Fine-tuning of nano-traps in a stable metal–organic framework for highly efficient removal of propyne from propylene†

Hui-Min Wen,^{‡,ab} Libo Li,^{‡,b} Rui-Biao Lin,^{ID b} Bin Li,^{ID *c} Bin Hu,^d Wei Zhou,^{ID e} Jun Hu,^{ID *a} and Banglin Chen,^{ID *b}

Despite tremendous efforts, precise control in the synthesis of porous materials with ideal nanocages for desired gas separation applications still remains a challenge. Microporous metal–organic frameworks (MOFs) have provided rich chemistry to enable precise control and design of structures, pore cavities, and functionalities at the molecular level. Here, we propose and design a microporous MOF (termed as ZJUT-1, ZJUT = Zhejiang University of Technology) with a fine-tuned nanocage, exhibiting the desired size, shape, and functionalities that are suitable for trapping a single propyne (C_3H_4) molecule. Adsorption and computational studies indicate that such optimized nanocages can not only reduce the uptake of propylene (C_3H_6), but also strengthen the C_3H_4 –host interactions through multiple hydrogen-bonding between $SiF_6^{2-}/-NH_2$ and C_3H_4 molecules. This material thus shows remarkably different C_3H_4 and C_3H_6 adsorption capacities, with the largest uptake ratio of 3.06 at 1 bar and 298 K, affording a very high selectivity (up to 70) for C_3H_4/C_3H_6 (1/99) separation. The actual breakthrough experiments demonstrate that ZJUT-1 can efficiently remove trace amounts of C_3H_4 from the important raw C_3H_4/C_3H_6 mixtures under ambient conditions with 0.19 mmol g^{-1} C_3H_4 uptake capacity to produce 99.9995% pure C_3H_6 .

Received 19th January 2018
Accepted 12th March 2018

DOI: 10.1039/c8ta00598b

rsc.li/materials-a

Introduction

Gas separation and purification through adsorbent-based separation technologies have attracted considerable attention from both academia and industry in recent years, which might enable a possible transition from traditional energy-intensive cryogenic distillation to energy-efficient adsorbent-based separation in the future.^{1–3} As an emerging type of porous material, microporous metal–organic frameworks (MOFs) have shown great potential as adsorbents for gas separation and

purification.^{4–7} Owing to their reticular chemistry and modular design, MOF materials have enabled the prospective design of target materials with great structural predictability and subsequently an accurate control of the pore size, shape, and functionality at the molecular level.^{8–10} Although thousands of MOFs have been prepared for diverse gas separation and purification in the past two decades, precise design of a pore cavity in MOFs that can specifically capture a single target gas molecule is rarely reported and still remains a challenge. To our knowledge, this adsorption phenomenon was only clearly realized in few MOFs with pre-designed single-molecule traps for CO_2 capture.¹¹ However, the design of porous materials with an ideal nanocage for single-molecular trapping of light hydrocarbons has been rarely reported yet.¹²

Propylene is one of the most prime olefin raw materials for petrochemical production, second in importance to ethylene. The capture and removal of a trace C_3H_4 impurity (typically 1%) from C_3H_6 is a very important separation to produce high-purity C_3H_6 in industry, while it remains very challenging due to their similar molecular sizes ($6.2 \times 3.8 \times 3.8 \text{ \AA}^3$ for C_3H_4 and $6.5 \times 4.0 \times 4.2 \text{ \AA}^3$ for C_3H_6).¹³ The only example was recently realized by Li *et al.* in a flexible robust MOF as a potential separating adsorbent.¹⁴ In this work, we aim to show how it is possible to elaborately design a nanocage within porous MOFs specifically for the capture of a single C_3H_4 molecule. As we know, C_3H_4 is a linear molecule, and four H atoms are distributed at two ends

^aCollege of Chemical Engineering, Zhejiang University of Technology, Zhejiang, 310014, P. R. China. E-mail: hjzjut@zjut.edu.cn

^bDepartment of Chemistry, University of Texas at San Antonio, One UTSA Circle, San Antonio, Texas 78249-0698, USA. E-mail: banglin.chen@utsa.edu; Fax: +1-210-458-7428

^cState Key Laboratory of Silicon Materials, Cyrus Tang Center for Sensor Materials and Applications, School of Materials Science and Engineering, Zhejiang University, Hangzhou, 310027, China. E-mail: bin.li@zju.edu.cn

^dKey Laboratory of Jiangxi Province for Persistent Pollutants Control and Resources Recycle, School of Environmental and Chemical Engineering, Nanchang Hangkong University, Nanchang 330063, China

^eNIST Center for Neutron Research, National Institute of Standards and Technology, Gaithersburg, MD 20899-6102, USA

† Electronic supplementary information (ESI) available: Stability tests, PXRD, TGA, GCMC simulations, and structural data. See DOI: 10.1039/c8ta00598b

‡ These authors have contributed equally to this work.

of the molecule. Recent studies have shown that the SIFSIX series are promising candidates for light hydrocarbon separation, because the SiF_6^{2-} anions have strong H-bonding interactions with the H atoms of hydrocarbon molecules to enhance their separation capacities.^{15,16} In particular, SIFSIX-3-M (M = Cu, Ni, and Zn) materials possess distinct CO_2 capture and $\text{C}_2\text{H}_2/\text{C}_2\text{H}_4$, and $\text{C}_3\text{H}_6/\text{C}_3\text{H}_8$ separation properties.^{17–19} Detailed structural studies have indicated that SIFSIX-3-Ni contains a lot of nanocages with a size of $7.5 \times 4.2 \times 4.2 \text{ \AA}^3$ that are separated by four SiF_6^{2-} anions (Fig. S1, ESI†).²⁰ This nanocage size and shape as well as decorated SiF_6^{2-} sites make it suitable to capture a single C_3H_4 molecule. Unfortunately, SIFSIX-3-Ni was found to adsorb large amounts of both C_3H_4 and C_3H_6 under ambient conditions (Fig. S2, ESI†) because the nanocage size is slightly larger than both gas molecules.

In order to reduce the C_3H_6 uptake, it is highly necessary to further fine-tune the nanocage size in this platform so that it can become more suitable for capture of a single C_3H_4 molecule while not for C_3H_6 . We anticipated that if a bigger ligand with functional sites (2-aminopyrazine, pyz-NH_2) instead of pyrazine (pyz) was used to construct the isorecticular ZJUT-1 (Fig. 1), the resulting microporous material was expected to exhibit a smaller nanocage with a contracted aperture size that might be more favorable to trap a single C_3H_4 molecule while limiting the passage of C_3H_6 to a certain degree. In addition, the immobilization of dual functionalities ($-\text{NH}_2$ and SiF_6^{2-}) into the nanocage can create a multi-binding environment to improve the specific recognition of C_3H_4 toward C_3H_6 . In this work, our experimental and simulation studies verify this hypothesis, and we herein report the structure, stability, adsorption isotherms, and experimental breakthrough curves of the activated material (ZJUT-1a). These data revealed that the contracted nanocages in ZJUT-1a with a size of $7.5 \times 3.7 \times 3.7 \text{ \AA}^3$ can efficiently reduce the C_3H_6 adsorption amount from $88 \text{ cm}^3 \text{ cm}^{-3}$ in SIFSIX-3-Ni to $28 \text{ cm}^3 \text{ cm}^{-3}$, while retaining the high uptake for the preferred C_3H_4 (89 vs. $91 \text{ cm}^3 \text{ cm}^{-3}$ in SIFSIX-3-Ni) attributed to the multi-binding environment, as

supported by computational studies. Therefore, this material exhibits the largest $\text{C}_3\text{H}_4/\text{C}_3\text{H}_6$ uptake ratio of 3.06 at 1 bar for the reported MOFs, and thus a high $\text{C}_3\text{H}_4/\text{C}_3\text{H}_6$ selectivity of ~ 70 for the 1/99 mixture. Highly efficient separation of C_3H_4 from the 1/99 $\text{C}_3\text{H}_4/\text{C}_3\text{H}_6$ mixture was further confirmed by experimental breakthrough tests.

Results and discussion

Reaction of pyz-NH_2 with NiSiF_6 in methanol solution at 85°C afforded a powder sample of $[\text{Ni}(\text{pyz-NH}_2)_2(\text{SiF}_6)]_n$ (ZJUT-1). The PXRD patterns of the as-synthesized and fully activated ZJUT-1 are shown in Fig. S4 (ESI†). The diffraction peak positions remain unchanged before and after sample activation, indicating that the ZJUT-1 framework is robust. The PXRD diagram of ZJUT-1 was found to match well with those of the SIFSIX-3 analogues reported previously (Fig. S5, ESI†), suggesting that the structure of ZJUT-1 should be isostructural to the net of the SIFSIX-3. Despite extensive attempts, we were not able to obtain single crystals for single-crystal X-ray diffraction studies and therefore structural determination was conducted by powder diffractometry.

On the basis of the PXRD data, we solved the structure of ZJUT-1 by using a direct method that can be found in our previous work (see ESI† for more details).²¹ Through indexing of the PXRD data, a monoclinic $B2$ space group was first identified for the ZJUT-1 crystal (note that the $B2$ setting, instead of the standard $C2$ setting, was selected in order to show the channel pore structure more straightforwardly in the unit cell). We thus further modeled its structure, using the same framework connection as SIFSIX-3-Ni. The simulated PXRD pattern of our structural model agrees excellently with the experimental data (Fig. 2a and S6, ESI†), strongly supporting its validity. Detailed structural information of ZJUT-1 is provided in Tables S1 and S2 (ESI†). Similar to the net of SIFSIX-3-Ni, this framework consists of two-dimensional nets based on pyz-NH_2 linkers and metal nodes that are pillared by SiF_6^{2-} anions in the third dimension

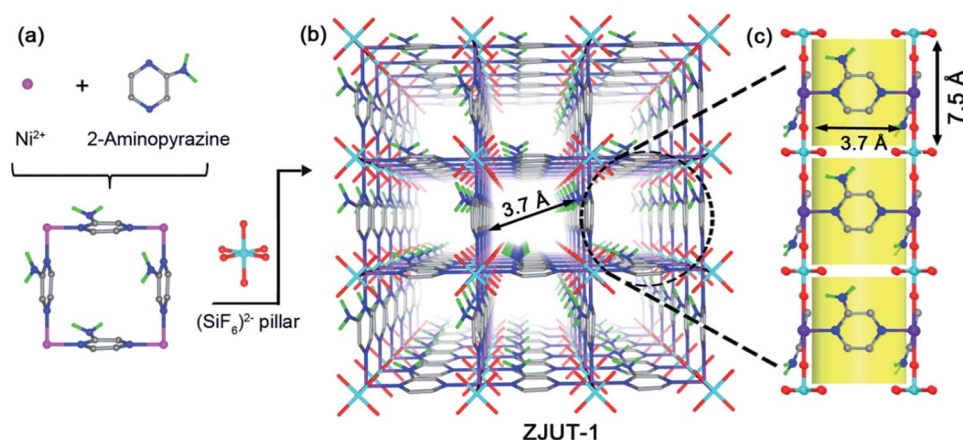


Fig. 1 Structure description of ZJUT-1. (a) Illustration of the square-shaped arrangement in the Ni-pyrazine (4,4') square grid that is further pillared by anion SiF_6^{2-} blocks to generate a 3D MOF, which is isostructural to the net in SIFSIX-3-Ni. (b) The channel structure of ZJUT-1 revealing an aperture size of $\approx 3.7 \text{ \AA}$, viewed along the b -axis. (c) The nanocages of ZJUT-1 with a size of $7.5 \times 3.7 \times 3.7 \text{ \AA}^3$ that are separated by four SiF_6^{2-} anions, when viewed along the a - and c -axes. Color code: F, red; Si, cyan; C, gray; H, green; N, blue; Ni, purple.

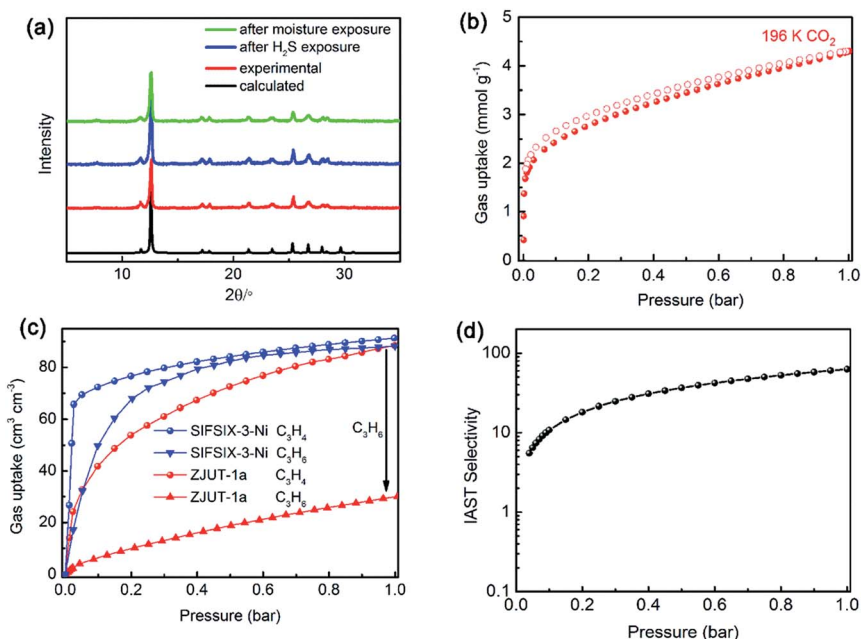


Fig. 2 (a) Powder X-ray diffraction experiments showing the stability of ZJUT-1 after exposure to moisture (85% humidity) and H₂S (5%). (b) Gas adsorption isotherms of ZJUT-1a for CO₂ at 196 K. (c) Adsorption isotherms of C₃H₄ and C₃H₆ for ZJUT-1a and SIFSIX-3-Ni at 298 K and 1 bar. (d) IAST selectivity of ZJUT-1a for C₃H₄/C₃H₆ (1/99, v/v) at 298 K.

to form three-dimensional (3D) nets (Fig. 1a and b). The use of amino-functionalized pyz-NH₂ instead of pyz as a linker offers: (i) a slight reduction of the aperture size due to the immobilized -NH₂ groups; and (ii) a certain degree of tilting of pyridine rings which are rotated by around 14 degrees with respect to the crystal axis (Fig. S7, ESI[†]). The SiF₆²⁻ pillars are interconnected with the -NH₂ group of pyridine through a strong hydrogen bonding of N-H...F (1.930 Å) to restrict the rotation of pyridine rings. As a result, the aperture size of ZJUT-1 was fine-tuned from 4.2 Å in SIFSIX-3-Ni to 3.7 Å. Most importantly, this material shows contracted cylindrical nanocages with a size of 7.5 × 3.7 × 3.7 Å³ that are separated by four SiF₆²⁻ anions, viewed along the *a*- and *c*-axes (Fig. 1c). This fine-tuned nanocage matches better with the size and shape of C₃H₄ (6.2 × 3.8 × 3.8 Å³) than C₃H₆ (6.5 × 4.0 × 4.2 Å³), making it an ideal single-molecule trap for the capture of a single C₃H₄ molecule. In addition, the immobilized dual functionalities of -NH₂ and SiF₆²⁻ groups are located around the cylindrical nanocages, which can create a multi-binding environment to strengthen the interactions with the C₃H₄ molecule. Thus, the combination of optimized nanocages and dual functionalities toward C₃H₄ in a single material may offer us great promise for selective separation of C₃H₄ from C₃H₄/C₃H₆ mixtures.

Prior to evacuating ZJUT-1 as a potential separating agent, we first examined its stability against moisture and H₂S by monitoring the PXRD patterns upon exposure to various humidity levels and H₂S concentrations (Fig. 2a). When the sample is exposed to air for more than 6 months, ZJUT-1 can retain its structural integrity (Fig. S8, ESI[†]). Further, during the exposure of ZJUT-1 to humidity from 20 to 85% or H₂S (up to 5%), we found that there is also no loss of crystallinity and no phase

change observed (Fig. S9 and S10, ESI[†]), indicating its excellent chemical stability to moisture and H₂S. The permanent porosity of the activated ZJUT-1a was confirmed by CO₂ adsorption measurements at 196 K with a CO₂ uptake of 4.1 mmol g⁻¹ (Fig. 2b). The Brunauer-Emmett-Teller (BET) surface area was calculated to be 222 m² g⁻¹, which is slightly lower than those of the SIFSIX-3 analogues (~250–350 m² g⁻¹).¹⁹

Single component gas adsorption isotherms for ZJUT-1a toward C₃H₄ and C₃H₆ were measured at 298 K and compared to those of SIFSIX-3-Ni, as shown in Fig. 2c. ZJUT-1a exhibits a high C₃H₄ uptake of 89 cm³ cm⁻³ at 298 K and 1 bar, which is comparable to that of SIFSIX-3-Ni and higher than that of ELM-12.¹⁴ However, the uptake of C₃H₆ increases very slowly following this pressure, with a low adsorption amount of 28 cm³ cm⁻³ at 298 K and 1 bar. This C₃H₆ value is much lower than that of SIFSIX-3-Ni (88 cm³ cm⁻³) because of the contracted nanocages of ZJUT-1a with respect to SIFSIX-3-Ni. The C₃H₄/C₃H₆ uptake ratio at 0.01 and 1.0 bar for ZJUT-1a was estimated to be 12.8 and 3.06, respectively, notably higher than those of SIFSIX-3-Ni (3.38 and 1.04) and the best-performing ELM-12 (2.73 and 1.92). These adsorption results combined with the excellent stability further endow this material with great potential for C₃H₄/C₃H₆ separation under ambient conditions.

We first utilized ideal adsorbed solution theory (IAST) to calculate the adsorption selectivity of ZJUT-1a for both 1/99 and 50/50 C₃H₄/C₃H₆ mixtures at room temperature. As shown in Fig. 2d, ZJUT-1a exhibits a high IAST selectivity for the 1/99 mixture, up to 70 at 1 bar and 298 K. In addition, the selectivity for the 50/50 mixture can reach 296 under ambient conditions (Fig. S12, ESI[†]). Both values are comparable to those of ELM-12 (84 and 279 for the 1/99 and 50/50 mixtures).

To gain further insight into the high C_3H_4 adsorption capacity of ZJUT-1a, grand canonical Monte Carlo (GCMC) simulations were performed to investigate the interactions between ZJUT-1a and the C_3H_4 molecule (see ESI† for details). As shown in Fig. 3a, due to the contracted nanocage ($7.5 \times 3.7 \times 3.7 \text{ \AA}^3$) in ZJUT-1a that matches well with C_3H_4 ($6.2 \times 3.8 \times 3.8 \text{ \AA}^3$), one unit cell of ZJUT-1a can only trap a single C_3H_4 molecule through multiple hydrogen bonding and van der Waals interactions between dual functionalities ($-NH_2$ and SiF_6^{2-}) with the C_3H_4 molecule (Fig. S13, ESI†). Detailed analyses revealed that three hydrogen atoms in the methyl group interact with four SiF_6^{2-} anions and one $-NH_2$ group through cooperative C-H...F and C-H...N-H-bonding (Fig. 3a). In addition, the hydrogen atom in the moiety of $H-C\equiv C$ is also bounded by four independent F atoms and one $-NH_2$ group (Fig. 3b), where the calculated distance of $C\equiv H\cdots F$ and $C\equiv H\cdots N$ is about 4.2 and 3.018 Å, respectively. Evidently, the immobilized SiF_6^{2-} and $-NH_2$ groups synergistically contribute to interact with the C_3H_4 molecule. The corresponding isosteric heat of adsorption (Q_{st}) for ZJUT-1a was calculated to be about 38 kJ mol^{-1} (Fig. S14, ESI†). This value is even higher than the Q_{st} for C_2H_2 discovered in the SIFSIX-3 series (21–31),^{19a} further confirming that ZJUT-1a has very strong binding affinity for C_3H_4 capture. Overall, we believe that it is the synergistic effect of the fine-tuned nanocage and dual functionalities make this material preferentially adsorb C_3H_4 over C_3H_6 significantly.

To examine the separation performance of ZJUT-1a in the actual C_3H_4/C_3H_6 separation, experimental breakthrough studies were conducted in a packed column of activated ZJUT-1a solid under a C_3H_4/C_3H_6 (1 : 99, v/v) gas mixture with a total flow of 2 mL min^{-1} at 298 K. As illustrated in Fig. 4a, highly efficient separation for the C_3H_4/C_3H_6 mixture was realized in ZJUT-1a. We found that the C_3H_6 gas first eluted through the adsorption bed to yield a polymer-grade gas, while C_3H_4 breakthrough did not occur until 130 min (the C_3H_4 concentration in the outlet below 5 ppm). The purity of C_3H_6 from the outlet effluent is $>99.9995\%$, which meets the requirement of $<5 \text{ ppm } C_3H_4$ in the downstream polymerization reaction. During this breakthrough process, the C_3H_6 production from the outlet effluent and the captured C_3H_4 amount for a given cycle were calculated to be 11.5 and 0.19 mmol g^{-1} , respectively.

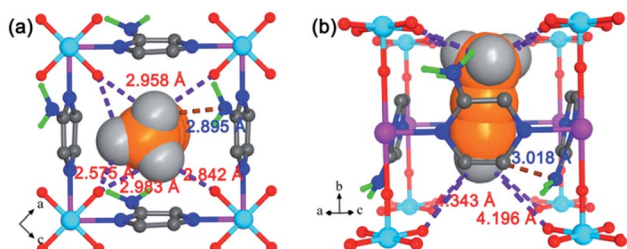


Fig. 3 The GCMC calculated C_3H_4 adsorption binding site in the nanocage of ZJUT-1a, indicating multiple H-bonding and van der Waals interactions between dual functionalities ($-NH_2$ and SiF_6^{2-}) and the C_3H_4 molecule. Color code: F, red; Si, cyan; C, gray; H, green; N, blue; Ni, purple; C (in C_3H_4): orange; H (in C_3H_4): white.

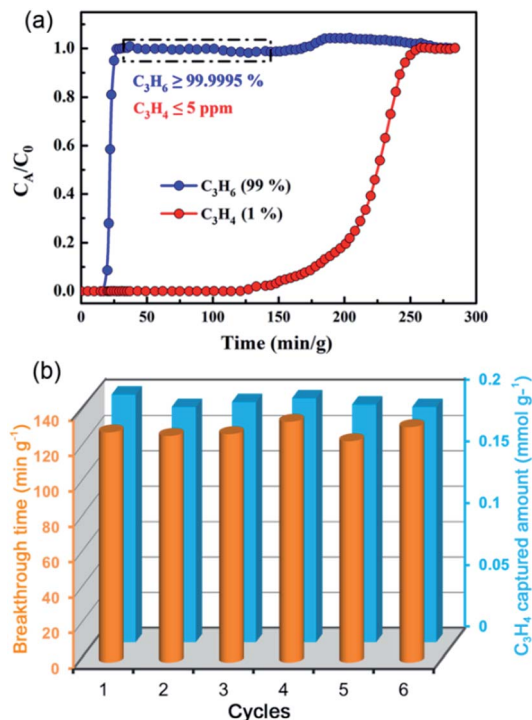


Fig. 4 (a) Experimental column breakthrough curves for a C_3H_4/C_3H_6 mixture containing 1% C_3H_4 (298 K, 1.01 bar) with a total flow of 2 mL min^{-1} in an absorber bed packed with ZJUT-1a. (b) The recyclability of ZJUT-1a in multiple mixed-gas column breakthrough tests.

In the practical C_3H_4 removal applications, the amenability to recycling and stability in the presence of moisture are also important. We thus performed multiple C_3H_4/C_3H_6 (1/99) mixed-gas column breakthrough tests to examine the preservation of the separation performance of ZJUT-1a (Fig. S16, ESI†). As shown in Fig. 4b and S17 (ESI†), the recycling measurements indicated that the breakthrough time and C_3H_4 capture capacity remain almost unchanged during 6 breakthrough experiments, confirming the good recyclability of this material for C_3H_4/C_3H_6 separation. In addition, the framework of ZJUT-1a remains stable after multiple C_3H_4 adsorption and breakthrough experiments, as revealed from the PXRD patterns of associated samples (Fig. S18, ESI†). To further confirm the moisture stability of this material, we measured the C_3H_4 adsorption properties of ZJUT-1a after the exposure of the sample to a humidity of 80% for 1 day. The results revealed that this activated sample retains its C_3H_4 adsorption capacity at 298 K (Fig. S19, ESI†), indicating its good stability toward moisture.

Conclusions

In summary, our foregoing findings demonstrated that it is feasible to precisely fine-tune the size, shape and functionality of the nanocage in MOFs to address important gas separations. Through using the larger 2-aminopyrazine to replace pyrazine as a linker, the resulting microporous MOF (ZJUT-1a) possesses a smaller nanocage with a contracted aperture size as well as multiple binding sites, compared to SIFSIX-3-Ni. Our results

indicate that such a fine-tuned nanocage is more suitable to serve as a single-molecule trap for the capture of a single C_3H_4 molecule over C_3H_6 , exhibiting a high C_3H_4/C_3H_6 selectivity that is even comparable to the previously best-performing MOF reported. ZJUT-1a thus can readily remove trace amounts of C_3H_4 from the 1/99 C_3H_4/C_3H_6 mixture, affording a high C_3H_4 uptake capacity of 0.19 mmol g^{-1} to produce 99.9995% pure C_3H_6 as demonstrated in the breakthrough experiments. In combination with the excellent recyclability and resistance to moisture and H_2S , ZJUT-1a represents bright promise as an adsorbent to be applied in industry for the removal of trace propyne from propylene.

Experimental section

General procedures and materials

All starting reagents and solvents were purchased from commercial companies and used without further purification. Thermogravimetric analyses (TGA) were carried out using a Shimadzu TGA-50 analyzer under a N_2 atmosphere with a heating rate of $5 \text{ }^\circ\text{C min}^{-1}$. Powder X-ray diffraction (PXRD) patterns were measured using a Rigaku Ultima IV diffractometer operated at 40 kV and 44 mA with a scan rate of 0.5 deg min^{-1} .

Synthesis of $[Cu(\text{pyz-NH}_2)_2(\text{SiF}_6)]_n$ (ZJUT-1)

ZJUT-1 was synthesized by the solvothermal reaction of nickel hexafluorosilicate (NiSiF_6 , 1 mmol) with 2-aminopyrazine (pyz-NH_2 , 2 mmol) in 20 mL methanol at $85 \text{ }^\circ\text{C}$. A light blue powder was obtained after 3 days, collected by filtration and then washed with methanol (65% yield based on pyz-NH_2).

Gas sorption measurements

A Micromeritics ASAP 2020 surface area analyzer was used to measure gas adsorption isotherms. To remove all the guest solvents in the framework, the fresh powder samples were first solvent-exchanged with dry methanol at least 10 times within two days, and evacuated at room temperature (298 K) for 24 h and additional 12 h at 323 K until the outgas rate was 5 mmHg min^{-1} prior to measurements. The sorption measurement was maintained at 196 K in a dry ice-acetone bath. An ice-water bath (slush) and a water bath were used for adsorption isotherms at 273 and 298 K, respectively.

Breakthrough experiments

The breakthrough curves were measured on a homemade apparatus for gas mixtures C_3H_4/C_3H_6 (1/99) at 298 K and 1.01 bar. In the separation experiment, ZJUT-1 (0.5233 g) particles with diameters of 200–300 μm were prepared and packed into a $\Phi 4 \times 150 \text{ mm}$ stainless steel column, and the column was activated under reduced pressure at 323 K overnight. The experimental set-up consisted of two fixed-bed stainless steel reactors. One reactor was loaded with the adsorbent, while the other reactor was used as a blank control group to stabilize the gas flow. The gas flows were controlled at the inlet using a mass flow meter at 2 mL min^{-1} , and a gas chromatograph (TCD-

Thermal Conductivity Detector, detection limit 0.1 ppm) continuously monitored the effluent gas from the adsorption bed. Prior to every breakthrough experiment, we activated the sample by flushing the adsorption bed with helium gas for 2 hours at 373 K. Subsequently, the column was allowed to equilibrate at the measurement rate before we switched the gas flow.

Conflicts of interest

There are no conflicts to declare.

Acknowledgements

This work was supported by an award AX-1730 from the Welch Foundation (BC), the National Natural Science Foundation of China (51672248, 21405139 and 21501088) and the Public Project of Zhejiang Province (2017C33172 and 2017C31049).

Notes and references

- (a) H. Furukawa, K. E. Cordova, M. O'Keeffe and O. M. Yaghi, *Science*, 2013, **341**, 6149; (b) S. Chu, Y. Cui and N. Liu, *Nat. Mater.*, 2017, **16**, 16; (c) G. Maurin, C. Serre, A. Cooper and G. Férey, *Chem. Soc. Rev.*, 2017, **46**, 3104.
- (a) J.-R. Li, J. Sculley and H.-C. Zhou, *Chem. Rev.*, 2012, **112**, 869; (b) K. Sumida, D. L. Rogow, J. A. Mason, T. M. McDonald, E. D. Bloch, Z. R. Herm, T.-H. Bae and J. R. Long, *Chem. Rev.*, 2012, **112**, 724; (c) K. Adil, Y. Belmabkhout, R. S. Pillai, A. Cadiau, P. M. Bhatt, A. H. Assen, G. Maurin and M. Eddaoudi, *Chem. Soc. Rev.*, 2017, **46**, 3402.
- (a) B. Li, H.-M. Wen, Y. Cui, W. Zhou, G. Qian and B. Chen, *Adv. Mater.*, 2016, **28**, 8819; (b) H. Wu, Q. Gong, D. H. Olson and J. Li, *Chem. Rev.*, 2012, **112**, 836; (c) J.-P. Zhang, Y.-B. Zhang, J.-B. Lin and X.-M. Chen, *Chem. Rev.*, 2012, **112**, 1001; (d) B. Li, H.-M. Wen, W. Zhou and B. Chen, *J. Phys. Chem. Lett.*, 2014, **5**, 3468.
- (a) R. W. Flaig, T. M. Osborn Popp, A. M. Fracaroli, E. A. Kapustin, M. J. Kalmutzki, R. M. Altamimi, F. Fathieh, J. A. Reimer and O. M. Yaghi, *J. Am. Chem. Soc.*, 2017, **139**, 12125; (b) D. A. Reed, B. K. Keitz, J. Oktawiec, J. A. Mason, T. Runcevski, D. J. Xiao, L. E. Darago, V. Crocella, S. Bordiga and J. R. Long, *Nature*, 2017, **550**, 96; (c) K.-J. Chen, D. G. Madden, T. Pham, K. A. Forrest, A. Kumar, Q.-Y. Yang, W. Xue, B. Space, J. J. Perry IV, J.-P. Zhang, X.-M. Chen and M. J. Zaworotko, *Angew. Chem., Int. Ed.*, 2016, **55**, 10268; (d) J. W. Yoon, H. Chang, S.-J. Lee, Y. K. Hwang, D.-Y. Hong, S.-K. Lee, J. S. Lee, S. Jang, T.-U. Yoon, K. Kwac, Y. Jung, R. S. Pillai, F. Faucher, A. Vimont, M. Daturi, G. Férey, C. Serre, G. Maurin, Y.-S. Bae and J.-S. Chang, *Nat. Mater.*, 2017, **16**, 526; (e) H. Sato, W. Kosaka, R. Matsuda, A. Hori, Y. Hijikata, R. V. Belosludov, S. Sakaki, M. Takata and S. Kitagawa, *Science*, 2014, **343**, 167.
- (a) Z. Niu, S. Fang, X. Liu, J.-G. Ma, S. Ma and P. Cheng, *J. Am. Chem. Soc.*, 2015, **137**, 14873; (b) T.-L. Hu, H. Wang, B. Li,

- R. Krishna, H. Wu, W. Zhou, Y. Zhao, Y. Han, X. Wang, W. Zhu, Z. Yao, S. Xiang and B. Chen, *Nat. Commun.*, 2015, **6**, 7328; (c) S. Yang, A. J. Ramirez-Cuesta, R. Newby, V. Garcia-Sakai, P. Manuel, S. K. Callear, S. I. Campbell, C. C. Tang and M. Schröder, *Nat. Chem.*, 2014, **7**, 121; (d) P.-Q. Liao, N.-Y. Huang, W.-X. Zhang, J.-P. Zhang and X.-M. Chen, *Science*, 2017, **356**, 1193; (e) D. Banerjee, H. Wang, Q. Gong, A. M. Plonka, J. Jagiello, H. Wu, W. R. Woerner, T. J. Emge, D. H. Olson, J. B. Parise and J. Li, *Chem. Sci.*, 2016, **7**, 759; (f) S. Xiang, Y. He, Z. Zhang, H. Wu, W. Zhou, R. Krishna and B. Chen, *Nat. Commun.*, 2012, **3**, 954; (g) Z. Hu, Y. Sun, K. Zeng and D. Zhao, *Chem. Commun.*, 2017, **53**, 8653.
- 6 (a) Q.-G. Zhai, X. Bu, C. Mao, X. Zhao, L. Daemen, Y. Cheng, A. J. Ramirez-Cuesta and P. Feng, *Nat. Commun.*, 2016, **7**, 13645; (b) L. Li, X. Wang, J. Liang, Y. Huang, H. Li, Z. Lin and R. Cao, *ACS Appl. Mater. Interfaces*, 2016, **8**, 9777; (c) C. Song, J. Hu, Y. Ling, Y. Feng, R. Krishna, D.-I. Chen and Y. He, *J. Mater. Chem. A*, 2015, **3**, 19417; (d) F. Luo, C. S. Yan, L. L. Dang, R. Krishna, W. Zhou, H. Wu, X. L. Dong, Y. Han, T.-L. Hu, M. O'Keeffe, L. L. Wang, M. B. Luo, R.-B. Lin and B. L. Chen, *J. Am. Chem. Soc.*, 2016, **138**, 5678; (e) N.-D. H. Gamage, K. A. McDonald and A. J. Matzger, *Angew. Chem., Int. Ed.*, 2016, **55**, 12099; (f) Z. Zhang, H. T. H. Nguyen, S. A. Miller, A. M. Ploskonka, J. B. DeCoste and S. M. Cohen, *J. Am. Chem. Soc.*, 2016, **138**, 920; (g) A. Hazra, S. Jana, S. Bonakala, S. Balasubramanian and T. K. Maji, *Chem. Commun.*, 2017, **53**, 4907.
- 7 (a) Y.-S. Bae, C. Y. Lee, K. C. Kim, O. K. Farha, P. Nickias, J. T. Hupp, S. T. Nguyen and R. Q. Snurr, *Angew. Chem., Int. Ed.*, 2012, **51**, 1857; (b) S.-J. Bao, R. Krishna, Y.-B. He, J.-S. Qin, Z.-M. Su, S.-L. Li, W. Xie, D.-Y. Du, W.-W. He, S.-R. Zhang and Y.-Q. Lan, *J. Mater. Chem. A*, 2015, **3**, 7361; (c) L. Du, Z. Lu, K. Zheng, J. Wang, X. Zheng, Y. Pan, X. You and J. Bai, *J. Am. Chem. Soc.*, 2013, **135**, 562; (d) D.-M. Chen, J.-Y. Tian, C.-S. Liu and M. Du, *Chem. Commun.*, 2016, **52**, 8413; (e) X. Zhao, J. G. Bell, S.-F. Tang, L. Li and K. Mark Thomas, *J. Mater. Chem. A*, 2016, **4**, 1353; (f) Y. Yuan, P. Cui, Y. Tian, X. Zou, Y. Zhou, F. Sun and G. Zhu, *Chem. Sci.*, 2016, **7**, 3751; (g) H.-R. Fu and J. Zhang, *Chem.-Eur. J.*, 2015, **21**, 5700.
- 8 (a) O. M. Yaghi, *J. Am. Chem. Soc.*, 2016, **138**, 15507; (b) W. Lu, Z. Wei, Z.-Y. Gu, T.-F. Liu, J. Park, J. Park, J. Tian, M. Zhang, Q. Zhang, T. Gentle III, M. Bosch and H.-C. Zhou, *Chem. Soc. Rev.*, 2014, **43**, 5561; (c) L. Liang, C. Liu, F. Jiang, Q. Chen, L. Zhang, H. Xue, H.-L. Jiang, J. Qian, D. Yuan and M. Hong, *Nat. Commun.*, 2017, **8**, 1233; (d) J.-P. Zhang, P.-Q. Liao, H.-L. Zhou, R.-B. Lina and X.-M. Chen, *Chem. Soc. Rev.*, 2014, **43**, 5789; (e) A. Schneemann, V. Bon, I. Schwedler, I. Senkowska, S. Kaskel and R. A. Fischer, *Chem. Soc. Rev.*, 2014, **43**, 6062.
- 9 (a) S. Furukawa, J. Reboul, S. Diring, K. Sumida and S. Kitagawa, *Chem. Soc. Rev.*, 2014, **43**, 5700; (b) Z. Chang, D.-H. Yang, J. Xu, T.-L. Hu and X.-H. Bu, *Adv. Mater.*, 2015, **27**, 5432; (c) Y. Yan, S. Yang, A. J. Blake and M. Schröder, *Acc. Chem. Res.*, 2014, **47**, 296; (d) H. Wang, Q.-L. Zhu, R. Zou and Q. Xu, *Chem*, 2017, **2**, 52; (e) H. Assi, G. Mouchaham, N. Steunou, T. Devic and C. Serre, *Chem. Soc. Rev.*, 2017, **46**, 3431; (f) Y. Li, K. Yao, Y. Zhu, Z. Deng, F. Yang, X. Zhou, G. Li, H. Wu, N. Nijem, Y. J. Chabal, Z. Lai, Y. Han, Z. Shi, S. Feng and J. Li, *Angew. Chem., Int. Ed.*, 2012, **51**, 1412.
- 10 (a) N. Ding, H. Li, X. Feng, Q. Wang, S. Wang, L. Ma, J. Zhou and B. Wang, *J. Am. Chem. Soc.*, 2016, **138**, 10100; (b) S. Yuan, L. Zou, J.-S. Qin, J. Li, L. Huang, L. Feng, X. Wang, M. Bosch, A. Alsalmé, T. Cagin and H.-C. Zhou, *Nat. Commun.*, 2017, **8**, 15356; (c) G. Cai and H.-L. Jiang, *Angew. Chem., Int. Ed.*, 2017, **56**, 563; (d) B. Li., H.-M. Wen, W. Zhou, J. Q. Xu and B. L. Chen, *Chem*, 2016, **1**, 557; (e) Q. Sun, C.-W. Fu, B. Aguila, J. A. Perman, S. Wang, H.-Y. Huang, F.-S. Xiao and S. Ma, *J. Am. Chem. Soc.*, 2018, **140**, 984.
- 11 (a) J.-R. Li, J. Yu, W. Lu, L.-B. Sun, J. Sculley, P. B. Balbuena and H.-C. Zhou, *Nat. Commun.*, 2013, **4**, 204; (b) J. A. Johnson, S. Chen, T. C. Reeson, Y.-S. Chen, X. C. Zeng and J. Zhang, *Chem.-Eur. J.*, 2014, **20**, 7632.
- 12 (a) Z. Bao, G. Chang, H. Xing, R. Krishna, Q. Ren and B. Chen, *Energy Environ. Sci.*, 2016, **9**, 3612; (b) Z. R. Herm, E. D. Bloch and J. R. Long, *Chem. Mater.*, 2014, **26**, 323.
- 13 (a) M. F. Friedrich, M. Lucas and P. Claus, *Catal. Commun.*, 2017, **88**, 73; (b) L. Li, R. Krishna, Y. Wang, J. Yang, X. Wang and J. Li, *J. Mater. Chem. A*, 2016, **4**, 751; (c) A. J. McCue, A. Guerrero-Ruiz, I. Rodríguez-Ramos and J. A. Anderson, *J. Catal.*, 2016, **340**, 10.
- 14 L. Li, R.-B. Lin, R. Krishna, X. Wang, B. Li, H. Wu, J. Li, W. Zhou and B. Chen, *J. Am. Chem. Soc.*, 2017, **139**, 7733.
- 15 (a) A. Cadiou, K. Adil, P. M. Bhatt, Y. Belmabkhout and M. Eddaoudi, *Science*, 2016, **353**, 137; (b) B. Li, X. Cui, D. O'Nolan, H.-M. Wen, M. Jiang, R. Krishna, H. Wu, R.-B. Lin, Y.-S. Chen, D. Yuan, H. Xing, W. Zhou, Q. Ren, G. Qian, M. J. Zaworotko and B. Chen, *Adv. Mater.*, 2017, **29**, 1704210.
- 16 (a) K.-J. Chen, H. S. Scott, D. G. Madden, T. Pham, A. Kumar, A. Bajpai, M. Lusi, K. A. Forrest, B. Space, J. J. Perry and M. J. Zaworotko, *Chem*, 2016, **1**, 753; (b) Z. Zhang, Q. Yang, X. Cui, L. Yang, Z. Bao, Q. Ren and H. Xing, *Angew. Chem., Int. Ed.*, 2017, **56**, 16282; (c) R.-B. Lin, L. Li, H. Wu, H. Arman, B. Li, R.-G. Lin, W. Zhou and B. Chen, *J. Am. Chem. Soc.*, 2017, **139**, 8022.
- 17 (a) P. Nugent, Y. Belmabkhout, S. D. Burd, A. J. Cairns, R. Luebke, K. Forrest, T. Pham, S. Ma, B. Space, L. Wojtas, M. Eddaoudi and M. J. Zaworotko, *Nature*, 2013, **495**, 80; (b) P. M. Bhatt, Y. Belmabkhout, A. Cadiou, K. Adil, O. Shekhah, A. Shkurenko, L. J. Barbour and M. Eddaoudi, *J. Am. Chem. Soc.*, 2016, **138**, 9301.
- 18 (a) A. Kumar, C. Hua, D. G. Madden, D. O'Nolan, K.-J. Chen, L.-A. J. Keane, J. J. Perry IV and M. J. Zaworotko, *Chem. Commun.*, 2017, **53**, 5946; (b) S. K. Elsaidi, M. H. Mohamed, H. T. Schaefer, A. Kumar, M. Lusi, T. Pham, K. A. Forrest, B. Space, W. Xu, G. J. Halder, J. Liu, M. J. Zaworotko and P. K. Thallapally, *Chem. Commun.*, 2015, **51**, 15530.

- 19 (a) X. Cui, K. Chen, H. Xing, Q. Yang, R. Krishna, Z. Bao, H. Wu, W. Zhou, X. Dong, Y. Han, B. Li, Q. Ren, M. J. Zaworotko and B. Chen, *Science*, 2016, **353**, 141; (b) S. K. Elsaidi, M. H. Mohamed, C. M. Simon, E. Braun, T. Pham, K. A. Forrest, W. Xu, D. Banerjee, B. Space, M. J. Zaworotko and P. K. Thallapally, *Chem. Sci.*, 2017, **8**, 2373.
- 20 (a) O. Shekhah, Y. Belmabkhout, K. Adil, P. M. Bhatt, A. J. Cairns and M. Eddaoudi, *Chem. Commun.*, 2015, **51**, 13595; (b) A. Kumar, D. G. Madden, M. Lusi, K.-J. Chen, E. A. Daniels, T. Curtin, J. J. Perry IV and M. J. Zaworotko, *Angew. Chem., Int. Ed.*, 2015, **54**, 14372.
- 21 G. Xu, B. Li, H. Wu, W. Zhou and B. Chen, *Cryst. Growth Des.*, 2017, **17**, 4795–4800.